ARTICLE

Check for updates

Phenotyping in clinical nutrition

Development and validation of bioelectrical impedance prediction equations estimating regional lean soft tissue mass in middle-aged adults

Luís B. Sardinha[1]✉, Gil B. Rosa[1], Megan Hetherington-Rauth[1], Inês R. Correia[1], João P. Magalhães[1], Analiza M. Silva[1] and Henry Lukaski[2]

BACKGROUND/OBJECTIVES: Bioelectrical impedance (BIA) whole-body and regional raw parameters have been used to develop prediction models to estimate whole-body lean soft tissue (LSTM), with less attention being given to the development of models for regional LSTM. Therefore, we aimed to develop and validate BIA-derived equations predicting regional LSTM against dual x-ray absorptiometry (DXA) in healthy adults.

SUBJECTS/METHODS: 149 adults were included in this cross-sectional investigation. Whole-body and regional LSTM were assessed by DXA, and raw bioelectrical parameters of distinct body regions were measured using a 50 kHz phase sensitive BIA analyzer. BIA-derived equations were developed using a stepwise multiple linear regression approach in 2/3 of the sample and cross-validated in the remaining sample.

RESULTS: Slopes and intercepts of predicted LSTM and DXA measured LSTM did not differ from 1 and 0, respectively, for each region ($p \geq 0.05$), with the exception for the trunk ($p < 0.05$). The BIA-derived equations exhibited a strong relationship ($p < 0.001$) between the predicted and measured LSTM for each of the following body regions: right and left arms ($R = 0.94$; $R = 0.96$), right and left legs ($R = 0.88$; $R = 0.88$), upper body ($R = 0.96$), lower body ($R = 0.89$), right and left sides of the body ($R = 0.94$; $R = 0.94$), and trunk ($R = 0.90$). Agreement analyses revealed no associations between the differences and the means of the predicted and DXA-derived LSTM.

CONCLUSION: The developed BIA-derived equations provide a valid estimate of regional LSTM in middle-aged healthy adults, representing a cost-effective and time-efficient alternative to DXA for the assessment and identification of LSTM imbalances in both clinical and sport-specific contexts.

European Journal of Clinical Nutrition (2023) 77:202–211; https://doi.org/10.1038/s41430-022-01224-0

INTRODUCTION

Body composition is an important element to consider when assessing individuals of a wide range of ages, given that age-specific patterns of changes occur naturally throughout the life span [1–3]. Skeletal muscle mass (SMM), for example, is a major predictor of physical function and survival rate later in life [4], and decreases throughout adulthood [5, 6], which leads to natural changes in whole-body lean soft tissue mass (LSTM) and appendicular LSTM (ALSTM). Thus, following body composition during adulthood will allow not only to target vulnerable groups exposed to SMM decline, but also to tailor effective interventions delaying this age-related deterioration.

Dual-energy X-ray absorptiometry (DXA) is a widely accepted method with high validity and reliability for the estimation of LSTM [7, 8] and has been shown to provide an adequate estimation of SMM [7]. Given the constraints regarding the use of this methodology (i.e., high cost and low portability), bioelectrical impedance analysis (BIA) has emerged as a more feasible alternative for body composition assessment [9–11]. The indirect estimation of body composition (i.e., fat-free mass (FFM) and LSTM) through BIA derives from measures of body tissue electrical conductivity and depends on the addition of biological and physiological variables to the prediction model [12]. Still, the accuracy of such prediction equations are device-specific and rely on the characteristics of the population in which they were developed [12].

The availability of tetrapolar BIA analyzers enables the estimation of regional body composition, which differs from the traditional whole-body technique [11]. To date, most measures of regional BIA are performed in a standing position on a platform embedded with stainless tetrapolar electrodes. Even though this is a convenient and applicable approach, several predicting errors resulting from inappropriate contact between the skin and the stainless electrodes

[1]Exercise and Health Laboratory, CIPER, Faculdade de Motricidade Humana, Universidade de Lisboa, Cruz-Quebrada, Portugal. [2]Department of Kinesiology and Public Health Education, Hyslop Sports Center, University of North Dakota, Grand Forks, ND, USA. ✉email: lsardinha@fmh.ulisboa.pt

Received: 20 June 2022 Revised: 3 October 2022 Accepted: 5 October 2022
Published online: 17 October 2022

Table 1. Characteristics of development and validation groups.

	Development group ($N = 100$)			Cross-validation group ($N = 49$)		
	Mean	**SD**	**Range**	**Mean**	**SD**	**Range**
Age (yrs)[a]	33.3	12.2	18–63	29.4	11.5	19–61
Females/Males (%)	51.0/49.0			53.1/46.9		
Caucasian/Black (%)	86.0/14.0			89.8/10.2		
Right/Left dominance (%)	88.0/12.0			95.9/4.1		
Weight (kg)	71.4	16.3	43.8–140.8	71.1	12.4	51.6–113.8
Height (cm)	168.0	9.5	146.4–190.8	169.4	9.0	150.5–186.9
BMI (kg/m^2)	25.2	4.7	17.2–46.7	24,8	4,6	18.6–47.2
FFM (kg)	51.6	12.0	32.9–100.6	52.6	10.2	36.7–78.3
FM (kg)	18.8	9.5	5.9–64.7	17.5	9.7	7.9–56.6
% FM	26.3	9.6	10.1–49.5	24.5	10.3	12.7–50.4
Left arm LSTM (kg)	2.8	1.0	1.3–6.3	2.8	0.8	1.6–4.8
Right arm LSTM (kg)	3.0	1.0	1.5–6.5	3.0	0.9	1.7–5.1
Left leg LSTM (kg)	8.6	2.1	5.3–16.4	8.9	2.1	5.8–14.7
Right leg LSTM (kg)	8.9	2.2	5.6–17.0	9.2	2.1	5.7–15.2
Trunk LSTM (kg)	24.6	5.6	15.7–49.0	24.9	4.4	17.7–37.7
Upper body LSTM (kg)	5.6	1.9	2.8–12.8	5.8	1.7	3.4–9.9
Lower body LSTM (kg)	17.4	4.4	11.0–33.4	18.1	4.2	11.6–29.9
Right body LSTM (kg)	24.1	5.9	15.1–48.0	24.7	5.0	16.6–37.5
Left body LSTM (kg)	23.7	5.8	14.4–47.3	24.1	5.0	16.4–36.5
Right arm *RI* (cm^2/Ω)	115.6	33.3	65.7–248.8	113.9	27.5	73.0–207.9
Right leg *RI* (cm^2/Ω)	122.7	27.4	79.5–227.4	122.2	22.1	79.0–167.2
Left arm *RI* (cm^2/Ω)	110.7	31.1	66.5–228.0	109.8	26.3	67.8–191.1
Left leg *RI* (cm^2/Ω)	119.4	27.0	64.1–221.4	119.8	21.9	81.0–167.1
Right trunk *RI* (cm^2/Ω)	1377.8	340.8	784.4–2459.8	1489.6	357.0	945.9–2544.2
Left trunk *RI* (cm^2/Ω)	1390.2	352.6	802.3–2493.5	1502.0	368.9	958.8–2523.0
Upper body *RI* (cm^2/Ω)	57.0	15.9	34.1–119.0	56.4	13.5	35.7–100.0
Lower body *RI* (cm^2/Ω)	60.7	13.3	39.0–111.7	60.7	10.9	40.3–81.8
Right body *RI* (cm^2/Ω)	56.8	13.8	37.1–112.0	56.4	11.3	37.7–85.6
Left body *RI* (cm^2/Ω)	54.9	13.2	36.2–106.4	55.0	11.2	36.6–84.4

BMI body mass index, *FFM* fat-free mass, *FM* fat mass, *LSTM* lean soft tissue mass, *RI* resistance index, *SD* standard deviation.
[a]Significant differences at the $p < 0.05$ level.

have been reported [13]. As an alternative, the use of a tetrapolar BIA approach with eight pre-gelled Ag/AgCl surface electrodes, while performed in a supine position, has been proposed to overcome some of these issues and compensates for differences in distinct body types. Currently, there is a research gap regarding the validation of regional BIA measurements for predicting DXA regional LSTM, with most of the equations being developed in specific populations, such as athletes [14, 15] and older adults [16–18]. Even though some recent equations predicting the overall LSTM of arms, legs and trunk have been developed in adults [19, 20], to the best of our knowledge, no previous investigations using tetrapolar BIA measurements with eight point electrodes have validated equations predicting DXA-derived LSTM of each body segment independently using healthy adults as the reference population. The present investigation aimed to develop and validate specific BIA-derived equations predicting regional DXA LSTM using a sample of adults varying in age, sex and body composition.

MATERIALS/METHODS AND SUBJECTS

Sample

This cross-sectional investigation included 149 adults (i.e., 77 women) with distinct body composition profiles (i.e., normal weight, overweight, and obese profiles). Participants with active pregnancy, implantable medical devices, amputated limbs, orthopedic prosthesis, skin wounds at the electrode placement sites, and under the administration of medication or clinical conditions with impact on water compartments or body cell mass were excluded. All data were collected between July and December 2020 at the Exercise and Health Laboratory, Faculty of Human Kinetics, University of Lisbon.

Anthropometry

Body weight and height were measured with participants wearing minimal clothing on an electronic scale with an integrated stadiometer (SECA 796 Hamburg, Germany) according to standardized procedures [21]. Body mass index was calculated as body weight divided by height squared.

Bioelectrical impedance analysis (BIA)

The impedance measurements were performed in the early morning following 12 h of fasting and after bladder voiding using a phase-sensitive single-frequency BIA (BIA 101 BIVA PRO, Akern S.R.L., Pisa, Italy), which applies an alternating current of 245 microamperes at 50 kHz. Prior to participation, participants were asked to maintain regular dietary habits, to refrain from exercising in the 24 h before to

Table 2. Developed prediction equations using development group ($N = 100$) for estimating DXA-derived LSTM from BIA and performance analysis of developed prediction equations using the cross-validation group ($N = 49$).

LSTM region	Development ($N = 100$)				Cross-validation ($N = 49$)[a]						
	equation[b]	R	Adj.R^2	SEE	Adj.R^2	PE	Bias[c]	LOA	Trend (r)[d]	Slope	Intercept
Left body (kg)	$9.016 + 0.399*RI_{LB} - 91.962*RI_{TE} + 1.229*$Sex (0 = F;1 = M)	0.950	0.900	1.823	0.875	1.729	0.15	−3.31; 3.61	−0.036	0.944	1.260
Right body (kg)	$0.461 + 0.273*RI_{RB} + 0.006*RI_{RT}$	0.947	0.894	1.902	0.880	1.693	0.14	−3.26; 3.54	−0.012	0.948	1.102
Lower body (kg)	$7.998 + 0.284*RI_{LwB} - 100.561*RI_{TE} + 1.559*$Sex (0 = F;1 = M)	0.947	0.894	1.413	0.785	1.886	−0.08	−3.78; 3.42	−0.235	0.983	0.091
Upper body (kg)	$1.560 + 0.102*RI_{UB} - 23.420*RI_{TE} + 0.717*$Sex (0 = F;1 = M)	0.959	0.918	0.550	0.910	0.497	0.01	−0.95; 0.99	−0.054	1.007	−0.051
Left leg (kg)	$4.756 + 0.067*RI_{LL} - 54.597*RI_{TE} + 0.901*$Sex (0 = F;1 = M)	0.938	0.876	0.751	0.775	0.960	−0.00	−1.80; 1.85	−0.259	1.021	−0.188
Right leg (kg)	$3.724 + 0.071*RI_{RL} - 46.197*RI_{TE} + 0.733*$Sex (0 = F;1 = M)	0.947	0.893	0.724	0.777	0.971	−0.11	-1.97; 1.76	−0.255	1.019	−0.061
Left arm (kg)	$0.676 + 0.026*RI_{LA} - 11.398*RI_{TE} + 0.346*$Sex (0 = F;1 = M)	0.956	0.911	0.285	0.907	0.251	0.01	−0.51; 0.52	−0.060	0.992	0.016
Right arm (kg)	$1.034 + 0.024*RI_{RA} - 12.272*RI_{TE} + 0.388*$Sex (0 = F;1 = M)	0.952	0.902	0.302	0.883	0.286	−0.02	−0.59; 0.55	−0.186	0.969	0.085
Trunk (kg)	$-10.039 + 0.015*RI_T + 160.945*RI_{TE}$	0.888	0.783	2.623	0.823	1.885	0.17	−3.85; 4.20	0.166	0.840	3.835

LSTM lean soft tissue mass, *Adj.*R^2 adjusted coefficient of determination, *SEE* standard error of estimation, *PE* pure error, *LOA* limits of agreement at 95% confidence interval, *F* female, *M* male, RI_{LB} left body resistance index, RI_{TE} resistance index of the ratio between trunk to extremities, RI_{RB}, right body resistance index, RI_{RT} right trunk resistance index, RI_{LwB} lower body resistance index, RI_{UB} upper body resistance index, RI_{LL} left leg resistance index, RI_{RL} right leg resistance index, RI_{LA} left arm resistance index, RI_{RA} right arm resistance index, RI_T mean trunk resistance index calculated as the mean of the right and left trunk resistance indexes, *VIF* variance inflation factor.

[a]Regression lines did not differ from the line of identity (i.e., slope and intercept did not differ from 1 and 0, respectively), with the exception for the trunk LSTM model.

[b]R^2 changed significantly ($p < 0.05$); no multicollinearity was observed (VIF < 5 and Tolerance > 0.20).

[c]No significant bias calculated as the mean difference between the new equation and the DXA region of interest.

[d]No significant association between the differences and the mean of the methods.

the assessment day, to not smoke in the 8 h before morning assessments, and to remove all metal accessories (e.g., ring, earrings, neckless, watches) before the assessment moment. After five minutes of rest to stabilize body fluids, the impedance measurements were performed with the subjects in the supine position with a leg opening of 45° compared to the median line of the body and the upper limbs positioned 30° away from the trunk.

Four injecting current electrodes were placed on the dorsal surface of both hands and feet, in the plane of the head of the third metacarpal and third metatarsal, respectively, while the remaining four electrodes (i.e., sensing electrodes) were placed on the dorsal surface of both wrists and tibia-tarsal joints, in the middle of an imaginary plane between the two styloid apophyses of each hand and in the middle of an imaginary plane between the two malleoli of each, respectively [14].

The resistance index (*RI*) of each body region was calculated as the full height (cm) squared divided by each regional *R* value (height^2/*R*) and used to represent the relative contribution of each body region to whole-body conductivity. In addition, the relative contribution of trunk and extremities to whole-body conductivity was calculated from the ratio between trunk and extremities *RI* [22]. The coefficient of variation in our laboratory for repeated within-day *R* and *Xc* measures was, respectively, 1.6% and 1.9% for the right arm, 1.9% and 1.7% for the left arm, 1.9% and 1.9% for the right leg, 1.1% and 2.0% for the left leg, 1.3% and 0.1% for the right trunk, and 3.4% and 0.7% for the left trunk.

Dual-energy X-ray absorptiometry (DXA)

Total and regional FFM were estimated on a DXA fan-beam densitometer (Hologic Explorer-W, fan-beam densitometer, software QDR for Windows version 12.4, Waltham, MA, USA) using a standardized protocol, with the same laboratory technician performing daily calibrations, consisting of scanning a step phantom with six fields of acrylic and aluminum of varying thickness and known absorptive properties to serve as an external standard for the analysis of different tissue components. In addition, the technician positioned the participants, performed the whole-body scans, and analyzed the data. Regional FFM was measured through partial analyses with Hologic APEX Version 3.3.0.1 analysis software, based on regions of interest defined by default. Regional LSTM was calculated by subtracting bone mineral content from FFM of each segment. The coefficient of variation of measurement in our laboratory for LSTM and ALSTM were 1.1% and 1.8%, respectively [23].

Statistical analysis

All analyses were performed using IBM SPSS Statistics, version 25 (SPSS Inc., Chicago, IL). Descriptive characteristics were presented as means, standard deviations and ranges (minimum-maximum). Normality was assessed using the Kolmogorov–Smirnov test ($n \geq 50$) for the development sample and the Shapiro–Wilk test ($n < 50$) for the validation sample. Differences between both samples were assessed using the Mann–Whitney U test (for continuous variables) and Fisher's Exact test (non-continuous variables). Statistical significance was set at $\alpha = 0.05$.

The prediction equations were established using a cross-validation method in which 100 participants (i.e., 2/3 of the sample) were selected in a random fashion using the basic random number generator in Excel (participants with the lowest 100 numbers were allocated to the development group), and used for equations development, while the remaining 49 (i.e., 1/3 of the sample) were used for equations validation. A sample size of 100 participants provided sufficient power to perform the development models to achieve a moderate effect size for the R^2, while considering the inclusion of four independent predictors (i.e., ≥2 participants per predictor rule) [24], a type-1 error of 5% and a power of 80%.

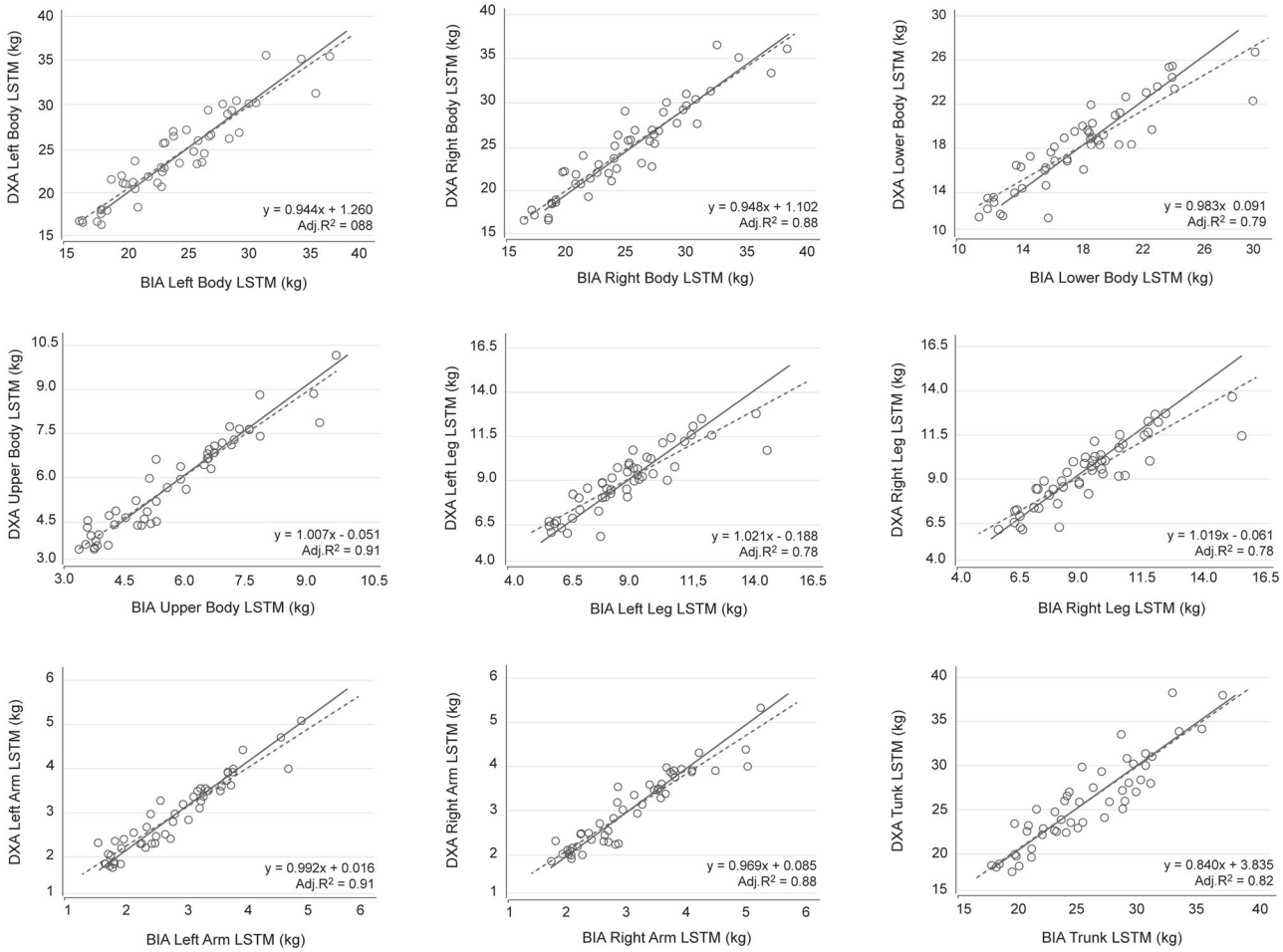

Fig. 1 Relationship between the measured and predicted LSTM. For all body regions are indicated the with line of identity (solid line) and the regression line of predicted and observed LSTM (dashed line). Adj.R2 adjusted coefficient of determination, BIA bioelectrical impedance, DXA dual X-ray absorptiometry, LSTM lean soft tissue mass, SEE standard error of estimation.

Equation development

A multiple linear regression approach with stepwise and backward selection procedures was used to develop equations for predicting DXA-derived LSTM of specific body regions using the development group. Predictor variables tested included sex, age, ethnicity, side dominance, standing height, sitting height, and raw BIA-derived measures (*Xc*, *R*, *RI*). Considering that no sex interactions were observed with the BIA parameters, this parameter was used as a predictor in the final models. The resulting equations were tested for multicollinearity using the variance inflation factor and, if multicollinearity was detected, the predictors with the lowest correlation with DXA-derived LSTM were eliminated. The model selection was based on the model coefficient of determination adjusted for the number of predictor variables in the model (i.e., adjusted R^2) and the standard error of estimation (SEE).

Equation cross-validation

The predicting model with the highest adjusted R^2 and the lowest SEE was selected for cross-validation analysis, and further compared with DXA-derived LSTM to assess the equality of the corresponding regression slopes and intercepts. To estimate the closeness of fit between BIA-predicted and DXA-measured LSTM of each segment, the 95% confidence intervals of each approach were assessed by testing the slope and intercept against the null values of 1 and 0, respectively.

The developed equations were applied to the validation group to predict the DXA-determined LSTM values. The paired sample t-test was used to compare mean values of BIA-predicted and DXA-measured LSTM in the validation group. The pure error (PE), which is the square root of the mean of squares of differences between the measured and predicted LSTM [25], was calculated to test the performance of the predictive equations. The Bland and Altman analysis [26] determined the limits of agreement (LOA) (mean difference ±2 SD) between BIA-derived and DXA-determined LSTM of all body regions. The statistical significance was set on p value <0.05.

RESULTS

There were no differences in the characteristics of the development and validation groups. All descriptive data is presented by group in Table 1.

Table 2 shows the developed prediction equations for estimating regional LSTM. In the regression analysis, sex, left body *RI* (RI_{LB}) and *RI* resulting from the ratio between trunk to extremities (RI_{TE}) explained 90% (Adj.$R^2 = 0.900$, SEE = 1.823) of the variance in DXA-measured left body LSTM, while right body *RI* (RI_{RB}) and right trunk *RI* (RI_{RT}) explained 89% (Adj.$R^2 = 0.894$, SEE = 1.902) of the variance in DXA-measured right body LSTM. For lower body LSTM prediction, sex, lower body *RI* (RI_{LwB}) and RI_{TE} explained 89% (Adj.$R^2 = 0.894$, SEE = 1.413) of the variance in DXA measured lower body LSTM,

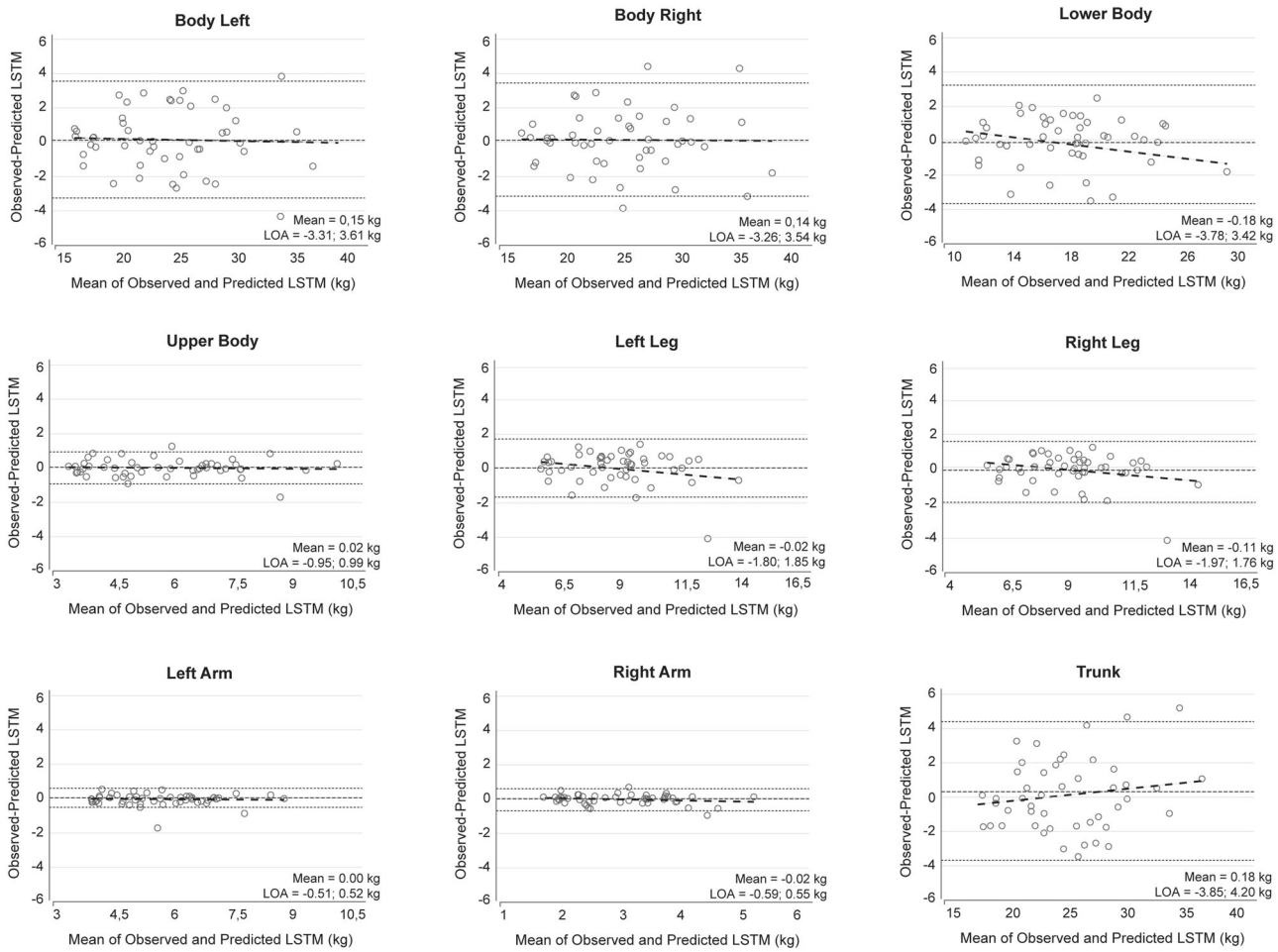

Fig. 2 Bland-Altman plots of the difference between observed and predicted LSTM. For all body regions are indicated the mean of the observed and predicted LSTM (long dashed line) and 95% LOA (short dashed line). LOA limits of agreement, LSTM lean soft tissue mass.

while sex, upper body *RI* (RI_{UB}) and RI_{TE} explained 92% (Adj.R^2 = 0.918, SEE = 0.550) of the variance in DXA measured upper body LSTM. For both right and left legs and arms, variables including sex, *RI* specific for each segment and RI_{TE} explained 89% (Adj.R^2 = 0.893, SEE = 0.724), 88% (Adj.R^2 = 0.876, SEE = 0.751), 90% (Adj.R^2 = 0.902, SEE = 0.302) and 91% (Adj.R^2 = 0.911, SEE = 0.285) of the variance in LSTM determined by DXA, respectively. The RI_{TE} and mean trunk *RI* (RI_T), calculated as the mean of the right and left trunk *RI*, explained 78% (Adj.R^2 = 0.783, SEE = 2.623) of the variance in trunk LSTM measured through DXA.

Figure 1 displays the relationship between predicted LSTM and DXA measured LSTM for each body segment. No differences were found between predicted and DXA-derived LSTM for all body regions, with exception to trunk LSTM ($p < 0.05$). In addition, strong relationships ($p < 0.001$) were observed between predicted and measured LSTM for upper and lower body (R = 0.96; R = 0.89), right and left sides of the body (R = 0.94; R = 0.94), right and left arms (R = 0.94; R = 0.96), right and left legs (R = 0.88; R = 0.88), and trunk (R = 0.90). In addition, slopes and intercepts of predicted LSTM and DXA-derived LSTM did not differ from 1 and 0, respectively, for each segment ($p \geq 0.05$), with the exception for the trunk model ($p < 0.05$).

Bland-Altman analyses (Fig. 2) revealed no associations between the differences and the means of the predicted and DXA-derived LSTM of the upper and lower body (r = 0.05, p = 0.72; r = −0.24, $p = 0.10$), right and left sides of the body (r = −0.01, $p = 0.93$; r = −0.04, $p = 0.81$), right and left arms (r = −0.19, $p = 0.20$; r = −0.06, $p = 0.68$), right and left legs (r = −0.26, $p = 0.08$; r = −0.26, $p = 0.07$) and trunk (r = 0.17, $p = 0.26$).

DISCUSSION

The present investigation led to the development and validation of BIA equations for predicting DXA LSTM of distinct body regions in a population of healthy adults. To date, no such equations are available for predicting regional LSTM derived from raw BIA parameters assessed using a tetrapolar BIA device with eight electrodes. This investigation offers multiple nonproprietary equations that accurately estimate LSTM of each body region independently and can be used in the future as a cost-effective and time-efficient alternative to DXA for the assessment of regional LSTM in adults with similar characteristics to the development sample.

The LSTM has been highlighted as an independent predictor of mobility and mortality across all ages [27]. Based on the construct that the largest portion of whole-body LSTM is primarily SMM and that approximately three-fourths of whole-body SMM is located in the limbs [28], a greater emphasis has been given to the assessment of ALSTM. Due to the influence of ALSTM on physical performance [29], a growing number of BIA prediction equations for upper and lower limbs LSTM have been developed in special populations (i.e., athletes and older adults), using whole-body [14] and raw BIA parameters [17] (see Table 3). Previous studies showed that BIA-derived equations to

Table 3. Summary of regional tetrapolar BIA (8-electrodes) findings.

Source	Study design	Subjects	Sample size and age	BIA device	Electrodes	Ref	Predictor variables	BIA-Pred vs Ref	Bias ($p < 0.05$)
Current investigation	Model develop, cross-validation	Healthy adults	M:72 F:77, 18 to 63 y	Akern	8 adhesive electrodes (distal positions)	DXA	Seg *RI*, sex	NS	None
Pietrobelli et al. [40]	Validation	Healthy adults	M:20 F:20, 29 ± 18 y	Tanita BC418	8 Contact	DXA	Device equations (unkown)	NS arms, legs, trunk LSTM & ALSTM	NA
Krimeler et al. [30]	Model develop, cross-validation	Children	M:162 F:171, 6 to 13 y	InBody 3.0	8 Contact	DXA	*RI*, sex, age, weight	NS arms legs LSTM	NA
Kim et al. [16]	Validation	Elderly	F: 129 81 ± 3 y	InBody 720	8 Contact	DXA	Device equations (unkown)	BIA < DXA, arms, legs & trunk LSTM, & ALSTM	Arms LSTM 1.4 vs 1.6 kg; Legs LSTM 4.5 vs 5.1 kg; Trunk LSTM 13.7 vs 16.4 kg; ALSTM 11.9 vs 13.4 kg
Lee et al. [41]	Validation	Elderly	M:42 F:35, 63 ± 6 y	Tanita BC418	8 Contact	DXA	Device equations (unkown)	NS, arms LSTM; BIA > DXA, legs LSTM	Legs LSTM 8.82 vs 7.9 kg
Buckinx et al. [10]	Validation	Healthy adults	M:106 F:113, 44 ± 19 y	In Body S10	8 Contact	DXA	Device equations (unkown)	BIA > DXA, ALSTM	ALSTM 9.19 vs 7.44 kg/m²
Esco et al. [15]	Validation	Athletes	F:45, 21 ± 2 y	In Body 720	8 Contact	DXA	Device equations (unkown)	NS, arms, legs & trunk LSTM	NA
Cheng et al. [42]	Validation	Athletes	M:48, 20 ± 1 y	Tanita BC418	8 Contact	DXA	Device equations (unkown)	NS, arms LSTM; BIA < DXA, legs LSTM; BIA > DXA, ALSTM	Legs LSTM 11.1 vs 11.9 kg; ALSTM 30.4 vs 28.7 kg
De Rui et al. [17]	Model develop, cross-validation	Elderly	M: 117 F:179, 71.6 y	Akern BIA ASE	8 adhesive electrodes (distal positions	DXA	Seg *RI*, *Xc*, sex, weight	NS, arms & legs LSTM	NA
Bosy-Westphal et al. [32]	Model develop, cross-validation	Healthy adults	M:70 F:66, 40 ± 12 y	Seca 515/514	8 Contact	DXA, MRI	Seg *RI*, *R*, *Xc*, sex, age, weight	NS, arms[24] & legs SMM[3]; BIA > MRI/DXA arms[1] & legs SMM[124]; BIA < MRI/DXA arms SMM[3]	Arms SMM 2.95 vs 3.11 kg[1], 3.25 vs 3.64 kg[3]; Legs SMM 10.97 vs 9.90 kg[1], 9.79 vs 8.48 kg[2], 10.45 vs 8.51 kg[4]
Wingo et al. [20]	Validation	Healthy adults	M:14 F:16, 32 ± 13 y	RJL Quantum IV	8 adhesive electrodes (distal positions)	DXA	Device equations (unknown -proprietary)	BIA > DXA arms & trunk LSTM	Arms LSTM 6.91 vs 5.93 kg; Trunk LSTM 29.58 vs 24.00 kg
Lee et al. [43]	Validation	Healthy adults	M:213 F:294, 6 ± 11 y	InBody 770	8 Contact	DXA	Device equations (unkown)	BIA > DXA ASMM	ASMM 18.2 vs 16.2 kg

Table 3. continued

Source	Study design	Subjects	Sample size and age	BIA device	Electrodes	Ref	Predictor variables	BIA-Pred vs Ref	Bias ($p < 0.05$)
Raymond et al. [44]	Validation	Athletes	M:44, 19 ± 1 y	InBody 770	8 Contact	DXA	Device equations (unkown)	BIA < DXA, legs FFM; NS, arms trunk FFM	Legs FFM 25.6 vs 31.0 kg
Brewer et al. [45]	Validation	Athletes	M:44 F:116 19 to 20 y	InBody 770	8 Contact	DXA	Device equations (unkown)	BIA < DXA arms & legs FFM	Arms FFM 6.3 vs 7.0 kg; Legs FFM 17.7 vs 21.5 kg
Moore et al. [19]	Validation	Healthy adults	M:76 F:103, 34 ± 15 y	RJL Quantum V	8 adhesive electrodes (distal positions)	DXA	Device equations (unknown -proprietary)	BIA > DXA, trunk & arms LSTM; BIA < DXA, legs LSTM; NS, ALSTM	Trunk LSTM 28.2 vs 27.2 kg; Arms LSTM 6.6 vs 5.9 kg; Legs LST 16.4 vs 17.0 kg
Sardinha et al. [14]	Model develop, cross-validation	Athletes	M: 168 F: 97, 22 ± 5 y	Akern BIA ASE	8 adhesive electrodes (distal positions)	DXA	*RI*, sex & weight	NS, arms & legs LSTM	NA
Schoenfeld et al. [46]	Validation; Training	Healthy men	M:21, 23 ± 3 y	InBody 720	8 Contact	DXA	Device equations (unkown)	BIA < DXA legs & trunk LSTM	RightLeg LSTM 10.1 vs 11.5 kg; LeftLeg LSTM 10.0 vs 11.3 kg; Trunk LSTM 30.8 vs 32.2 kg
Tinsley et al. [47]	Model develop, cross-validation	Healthy adults	F:103, M:76, 34 ± 15 y	RJL Quantum V	8 adhesive electrode (distal positions)	DXA	Device equations (unknown -proprietary)	BIA > DXA arms, & trunk LSTM & ALSTM; BIA < DXA legs	Arms LSTM 6.6 vs 5.9 kg Legs LSTM 16.4 vs 17.0 kg Trunk LSTM 28.2 vs 27.3 kg ALSTM 23.9 vs 22.7 kg

ADP air displacement plethysmography, *ALSTM* appendicular lean soft tissue mass, *ASMM* appendicular skeletal muscle mass, *BIA* bioelectrical impedance, *DXA* dual x-ray absorptiometry, *ECF* extracellular fluid, *FFM* fat-free mass, *LSTM* lean soft tissue mass, *NA* not applicable, *NS* not significant, *R* resistance, *RI* resistance index, *SMM* skeletal muscle mass, *Xc* reactance.
Ethnicity: [1]Caucasian, [2]Asian, [3]Afro-American, [4]Hispanic.

predict ALSTM in athletes accounted for 84 to 89% of the variability in upper limbs LSTM and for 81 to 93% of the variability in lower limbs LSTM as measured by DXA [14]. In addition, a similar variance was found in older adults with BIA prediction equations accounting for 83–90% of the variability in upper limbs LSTM and for 83 to 85% of the variability in lower limbs LSTM assessed through DXA [20]. Even though the BIA prediction equations emerging from the present investigation accounted for a similar variance in upper limbs LSTM as those in athletes and older adults (88 to 91%), the percent of variability in lower limbs LSTM was slightly lower (78%). Since the validation sample included adults from a wide spectrum of ages and body composition profiles, the estimation of body composition through BIA-derived parameters may have contributed to inconsistent relations between lower limbs LSTM and bioelectrical resistance in some individuals. Although there were no statistical differences between observed and predicted LSTM in the lower limbs, the BIA models for lower limbs LSTM exhibited wide LOA and high PE, similar to findings reported in athletes [14]. Although the use of eight electrodes is expected to perform better compared to using a traditional tetrapolar BIA approach [30], the wide LOA reported in the present investigation may be mostly explained by the high levels of individual variability in regional LSTM within our sample [30]. For instance, our findings revealed that in almost all body regions, with the exception of the lower body, the agreement between DXA and BIA predicted LSTM fell outside of the 95% limits for some cases. Therefore, even though caution should be taken when using these equations to estimate regional LSTM at the individual level (due to high individual variability), these equations have shown to provide accurate estimations when used at the group level.

Since the main component of whole-body and appendicular LSTM is SMM, an important health and nutritional indicator particularly during older adulthood [29], most of BIA-derived equations predicting ALSTM have been developed for the older adult population using DXA as the reference method [17, 18]. By contrast, only few investigations using multifrequency or tetrapolar BIA measurements with eight-point electrodes have developed and validated BIA-derived equations predicting ALSTM assessed by DXA using a sample of healthy adults [19, 20]. Even so, no studies have developed equations predicting DXA-derived ALSTM of each body segment independently in adults. Thus, by developing and validating BIA-derived equations predicting LSTM for each limb, as well as LSTM of other underexplored body regions (e.g., upper and lower body), our investigation makes a significant contribution to research in the field of body composition.

It is important to highlight that among all predictor variables considered, regional *RI* was the only bioelectrical parameter to fit in all equations, suggesting a predominant role of this parameter in estimating LSTM [17]. This finding reinforces the previous evidence highlighting *RI* as the main contributor of LSTM (with a variance accounting for approximately 80-90%) [17, 31]. Even though additional raw BIA variables, such as *R* and *Xc*, have been considered when estimating regional LSTM [17, 32], as presented in Table 3, these variables did not significantly contribute to our models and were not included. This is somewhat surprising, considering that *Xc*, for example, is mainly related to the capacitance function of the cell membranes, including skeletal muscle cells, which are the main component of LSTM [12]. Nevertheless, our findings concur with previous available evidence suggesting that *Xc* does not contribute [14] or contributes very little [17] to the prediction of regional LSTM in adults, regardless of their BMI, possibly due to a greater stabilization of *Xc* during this period of life [33]. Therefore, this parameter should rather be considered and included as a predictor of regional LSTM in children and older adult populations [12].

Despite the validity of our newly developed equations, there are some limitations that are worth noting. First, the use of DXA as the reference method is expected to overestimate specific parameters (i.e., SMM), when compared to other reference methods (i.e., computed tomography) [34]. This difference relies on the fact that LSTM is a heterogeneous body component at the molecular level of analysis, composed by water, protein, soft-minerals, and glycogen [35], and was used as a surrogate for assessing SMM, a tissue-level component. As a consequence, other tissue-level components such as skin, blood vessels, connective tissue and fat-free adipose tissue may have not been discriminated from SMM when using LSTM as a predictor [36]. Nevertheless, DXA measured LSTM in the limbs has been found to be significantly interrelated to SMM and is considered an accurate method to assess both appendicular and whole-body composition [37]. In addition, the development of equations that include the trunk segment may be a limitation, considering that significant differences were found between the observed and predicted values of LSTM in this segment. Even though the trunk represents approximately 50% of the body mass, it only has a slight contribution (5–12%) to whole-body resistance. This phenomenon can be attributed to the trunk geometry (i.e., short length and large diameter) and fluid compartmentalization [38], which have been shown to adversely compromise the estimation of trunk impedance components using tetrapolar BIA devices [39]. Although a strength of our study was the development and validation of our equations in a diverse, heterogenous group of adults, which allows our equations to be applied to participants from a wide spectrum of ages and body composition profiles, our equations may not be applicable to populations with different characteristics (e.g., children, older adults, people with chronic diseases, and other ethnicities) and when other BIA devices and approaches (frequencies different from 50 Hz) are considered. Finally, the estimation of regional body composition using whole-body raw BIA parameters may contribute to inconsistent relations between DXA regional LSTM and the BIA-derived parameters. Thus, to maximize BIA estimations, a major strength of our investigation was the use of a tetrapolar BIA device, which allowed for the assessment of regional raw BIA parameters. However, given that some tetrapolar BIA devices do not discriminate the boundaries of the body regions of interest, it remains unclear whether region of interest used by BIA devices can be comparable to the DXA regions defined by default according to the manufacturer.

In summary, BIA-derived equations predicting LSTM of distinct body regions were developed and validated using an independent sample of healthy adults. These equations have the potential to be applied to monitor changes in regional LSTM that naturally occur throughout adulthood, and to follow the changing patterns resulting from health-related programs. Further research is needed to examine the validity of these equations in different multi-ethnic populations.

DATA AVAILABILITY

Data are available from the corresponding author on reasonable request.

REFERENCES

1. Kirchengast S. Gender Differences in Body Composition from Childhood to Old Age: An Evolutionary Point of View. J Life Sci. 2010;2:1–10.
2. Janssen I, Heymsfield SB, Wang ZM, Ross R. Skeletal muscle mass and distribution in 468 men and women aged 18-88 yr. J Appl Physiol (1985) 2000;89:81–8.
3. Sillanpää E, Cheng S, Häkkinen K, Finni T, Walker S, Pesola A, et al. Body composition in 18- to 88-year-old adults—comparison of multifrequency bioimpedance and dual-energy X-ray absorptiometry. Obesity 2014;22:101–9.
4. Bosy-Westphal A, Müller MJ. Identification of skeletal muscle mass depletion across age and BMI groups in health and disease - there is need for a unified definition. Int J Obes. 2015;39:379–86.

5. Lexell J, Henriksson-Larsén K, Winblad B, Sjöström M. Distribution of different fiber types in human skeletal muscles: Effects of aging studied in whole muscle cross sections. Muscle Nerve. 1983;6:588–95.
6. Volpi E, Nazemi R, Fujita S. Muscle tissue changes with aging. Curr Opin Clin Nutr Metab Care. 2004;7:405–10.
7. Prior BM, Cureton KJ, Modlesky CM, Evans EM, Sloniger MA, Saunders M, et al. In vivo validation of whole body composition estimates from dual-energy X-ray absorptiometry. J Appl Physiol (1985) 1997;83:623–3.
8. Fuller NJ, Laskey MA, Elia M. Assessment of the composition of major body regions by dual-energy X-ray absorptiometry (DEXA), with special reference to limb muscle mass. Clin Physiol. 1992;12:253–66.
9. Kyle UG, Bosaeus I, De Lorenzo AD, Deurenberg P, Elia M, Manuel Gómez J, et al. Bioelectrical impedance analysis-part II: utilization in clinical practice. Clin Nutr. 2004;23:1430–53.
10. Buckinx F, Reginster J-Y, Dardenne N, Croisiser J-L, Kaux J-F, Beaudart C, et al. Concordance between muscle mass assessed by bioelectrical impedance analysis and by dual energy X-ray absorptiometry: a cross-sectional study. BMC Musculoskelet Disord. 2015;16:60.
11. Kyle UG, Bosaeus I, De Lorenzo AD, Deurenberg P, Elia M, Gómez JM, et al. Bioelectrical impedance analysis-part I: review of principles and methods. Clin Nutr. 2004;23:1226–43.
12. Beaudart C, Bruyère O, Geerinck A, Hajaoui M, Scafoglieri A, Perkisas S, et al. Equation models developed with bioelectric impedance analysis tools to assess muscle mass: A systematic review. Clin Nutr ESPEN. 2020;35:47–62.
13. Lukaski HC, Siders WA. Validity and accuracy of regional bioelectrical impedance devices to determine whole-body fatness. Nutrition 2003;19:851–7.
14. Sardinha LB, Correia IR, Magalhães JP, Júdice PB, Silva AM, Hetherington-Rauth M. Development and validation of BIA prediction equations of upper and lower limb lean soft tissue in athletes. Eur J Clin Nutr. 2020;74:1646–52.
15. Esco MR, Snarr RL, Leatherwood MD, Chamberlain NA, Redding ML, Flatt AA, et al. Comparison of total and segmental body composition using DXA and multifrequency bioimpedance in collegiate female athletes. J Strength Cond Res. 2015;29:918–25.
16. Kim M, Kim H. Accuracy of segmental multi-frequency bioelectrical impedance analysis for assessing whole-body and appendicular fat mass and lean soft tissue mass in frail women aged 75 years and older. Eur J Clin Nutr. 2013;67:395–400.
17. De Rui M, Veronese N, Bolzetta F, Berton L, Carraro S, Bano G, et al. Validation of bioelectrical impedance analysis for estimating limb lean mass in free-living Caucasian elderly people. Clin Nutr. 2017;36:577–84.
18. Scafoglieri A, Clarys JP, Bauer JM, Verlaan S, Van Malderen L, Vantieghem S, et al. Predicting appendicular lean and fat mass with bioelectrical impedance analysis in older adults with physical function decline - The PROVIDE study. Clin Nutr. 2017;36:869–75.
19. Moore ML, Benavides ML, Dellinger JR, Adamson BT, Tinsley GM. Segmental body composition evaluation by bioelectrical impedance analysis and dual-energy X-ray absorptiometry: Quantifying agreement between methods. Clin Nutr. 2020;39:2802–10.
20. Wingo BC, Barry VG, Ellis AC, Gower BA. Comparison of segmental body composition estimated by bioelectrical impedance analysis and dual-energy X-ray absorptiometry. Clin Nutr ESPEN. 2018;28:141–7.
21. Lohman TG, Roche AF, Martorell R Anthropometric standardization reference manual. Champaign, IL: Human Kinetics Books; 1988.
22. Bosy-Westphal A, Schautz B, Later W, Kehayias JJ, Gallagher D, Müller MJ. What makes a BIA equation unique? Validity of eight-electrode multifrequency BIA to estimate body composition in a healthy adult population. Eur J Clin Nutr. 2013;67:S14–21.
23. Silva AM, Santos DA, Matias CN, Rocha PM, Petroski EL, Minderico CS, et al. Changes in regional body composition explain increases in energy expenditure in elite junior basketball players over the season. Eur J Appl Physiol. 2012;112:2727–37.
24. Austin PC, Steyerberg EW. The number of subjects per variable required in linear regression analyses. J Clin Epidemiol. 2015;68:627–36.
25. Chumlea WC, Sun S, editors. Bioelectrical Impedance Analysis.: Human Body Composition 2005.
26. Bland JM, Altman DG. Statistical methods for assessing agreement between two methods of clinical measurement. Lancet (Lond, Engl). 1986;1:307–10.
27. Prado CM, Heymsfield SB. Lean tissue imaging: a new era for nutritional assessment and intervention. J Parenter Enter Nutr. 2014;38:940–53.
28. Lee RC, Wang Z, Heo M, Ross R, Janssen I, Heymsfield SB. Total-body skeletal muscle mass: development and cross-validation of anthropometric prediction models. Am J Clin Nutr. 2000;72:796–803.
29. Ylihärsilä H, Kajantie E, Osmond C, Forsén T, Barker DJP, Eriksson JG. Birth size, adult body composition and muscle strength in later life. Int J Obes. 2007;31:1392–9.
30. Kriemler S, Puder J, Zahner L, Roth R, Braun-Fahrländer C, Bedogni G. Cross-validation of bioelectrical impedance analysis for the assessment of body composition in a representative sample of 6- to 13-year-old children. Eur J Clin Nutr. 2009;63:619–26.
31. Toselli S, Campa F, Matias CN, de Alencar Silva BS, Dos Santos VR, Maietta Latessa P, et al. Predictive equation for assessing appendicular lean soft tissue mass using bioelectric impedance analysis in older adults: Effect of body fat distribution. Exp Gerontol. 2021;150:111393.
32. Bosy-Westphal A, Jensen B. Quantification of whole-body and segmental skeletal muscle mass using phase-sensitive 8-electrode medical bioelectrical impedance devices. 2017;71:1061–7.
33. Bosy-Westphal A, Danielzik S, Dörhöfer R-P, Piccoli A, Müller MJ. Patterns of bioelectrical impedance vector distribution by body mass index and age: implications for body-composition analysis. Am J Clin Nutr. 2005;82:60–8.
34. Bredella MA, Ghomi RH, Thomas BJ, Torriani M, Brick DJ, Gerweck AV. et al. Comparison of DXA and CT in the assessment of body composition in premenopausal women with obesity and anorexia nervosa. Obesity (Silver Spring. Md). 2010;18:2227–33.
35. Wang ZM, Pierson RN Jr., Heymsfield SB. The five-level model: a new approach to organizing body-composition research. Am J Clin Nutr. 1992;56:19–28.
36. Pietrobelli A, Formica C, Wang Z, Heymsfield SB. Dual-energy X-ray absorptiometry body composition model: review of physical concepts. Am J Physiol. 1996;271:E941–51.
37. Sergi G, De Rui M, Stubbs B, Veronese N, Manzato E. Measurement of lean body mass using bioelectrical impedance analysis: a consideration of the pros and cons. Aging Clin Exp Res. 2017;29:591–7.
38. Buchholz AC, Bartok C, Schoeller DA. The validity of bioelectrical impedance models in clinical populations. Nutr Clin Pr. 2004;19:433–46.
39. Shafer KJ, Siders WA, Johnson LK, Lukaski HC. Validity of segmental multiple-frequency bioelectrical impedance analysis to estimate body composition of adults across a range of body mass indexes. Nutrition 2009;25:25–32.
40. Pietrobelli A, Rubiano F, St-Onge MP, Heymsfield SB. New bioimpedance analysis system: improved phenotyping with whole-body analysis. Eur J Clin Nutr. 2004;58:1479–84.
41. Lee L-C, Hsieh K-C, Wu C-S, Chen Y-J, Chiang J, Chen Y-Y. Validity of Standing Posture Eight-electrode Bioelectrical Impedance to Estimate Body Composition in Taiwanese Elderly. Int J Gerontol. 2014;8:137–42.
42. Cheng MF, Chen YY, Jang TR, Lin WL, Chen J, Hsieh KC. Total body composition estimated by standing-posture 8-electrode bioelectrical impedance analysis in male wrestlers. Biol Sport. 2016;33:399–405.
43. Lee SY, Ahn S, Kim YJ, Ji MJ, Kim KM, Choi SH, et al. Comparison between Dual-Energy X-ray Absorptiometry and Bioelectrical Impedance Analyses for Accuracy in Measuring Whole Body Muscle Mass and Appendicular Skeletal Muscle Mass. Nutrients. 2018;10:738.
44. Raymond CJ, Dengel DR, Bosch TA. Total and Segmental Body Composition Examination in Collegiate Football Players Using Multifrequency Bioelectrical Impedance Analysis and Dual X-ray Absorptiometry. J Strength Cond Res. 2018;32:772–82.
45. Brewer GJ, Blue MNM, Hirsch KR, Peterjohn AM, Smith-Ryan AE. Appendicular Body Composition Analysis: Validity of Bioelectrical Impedance Analysis Compared With Dual-Energy X-Ray Absorptiometry in Division I College Athletes. J Strength Cond Res. 2019;33:2920–5.
46. Schoenfeld BJ, Nickerson BS, Wilborn CD, Urbina SL, Hayward SB, Krieger J, et al. Comparison of Multifrequency Bioelectrical Impedance vs. Dual-Energy X-ray Absorptiometry for Assessing Body Composition Changes After Participation in a 10-Week Resistance Training Program. J Strength Cond Res. 2020;34:678–88.
47. Tinsley GM, Moore ML, Rafi Z, Griffiths N, Harty PS, Stratton MT, et al. Explaining Discrepancies Between Total and Segmental DXA and BIA Body Composition Estimates Using Bayesian Regression. J Clin Densitom. 2021;24:294–307.

ACKNOWLEDGEMENTS

We would like to express our gratitude to the participants for their contribution in the present investigation. This investigation was conducted at Interdisciplinary Center of the Study of Human. Performance (CIPER), Faculty of Human Kinetics of the University of Lisbon, and supported by. fellowships from the Portuguese Foundation for Science and Technology (grant to GBR: 2020.07856.BD; grant to IRC: SFRH/BD/149394/2019; grant within the unit I&D 472 -UIDB/00447/2020).

AUTHOR CONTRIBUTIONS

LBS conceived and planned the experiments. GBR, JPM and IRC carried out the experiments and data collection. GBR, MHR and AMS did the data analysis. LBS, GBR, AMS and HL contributed to the interpretation of the results. LBS took the lead in writing the manuscript. All authors provided critical feedback and helped shape the research, analysis, and manuscript.

COMPETING INTERESTS

The authors declare no competing interests.

ETHICAL APPROVAL

The investigation protocol was approved by the Ethics Committee of the Faculty of Human Kinetics (12/2020), University of Lisbon, and conducted in accordance with the Declaration of Helsinki. All participants provided written informed consent before participation.

ADDITIONAL INFORMATION

Correspondence and requests for materials should be addressed to Luís B. Sardinha.